future workers who may study such systems. It is worth noting that in order to stabilize approximately one-half of the methyl iodide resulting from the association of $CH_3 + I$ at 600°K., about 1 atm. pressure is required. Similar calculations[12b] have been done for methane formed by $H + CH_3$ which satisfied the existing experimental data and predicted that $S/D = 1$ at a pressure of about 400 cm. at 673°K.

Pulse Radiolysis of Gaseous Argon–Oxygen Solutions. Rate Constant for the Ozone Formation Reaction[1a]

Myran C. Sauer, Jr., and Leon M. Dorfman[1b]

Contribution from Argonne National Laboratory, Argonne, Illinois.
Received May 6, 1965

The pulse-radiolysis method has been used to study the kinetics of ozone formation in gaseous argon–oxygen solutions. The absolute rate constant for the reaction $O + O_2 + Ar = O_3 + Ar$ *was found to be* $(0.83 \pm 0.08) \times 10^8\ M^{-2}\ sec.^{-1}$ *at 23°.*

Introduction

The extension of the technique of pulse radiolysis[2] to the gas phase has been described in a preliminary report.[3] In this paper we present the details of the experimental determination of the rate constant of the reaction 1 by direct observation of the ozone formation curve in the pulse radiolysis of gaseous argon–oxygen solutions.

$$O + O_2 + Ar = O_3 + Ar \qquad (1)$$

The reaction of oxygen atoms with molecular oxygen has been the subject of numerous investigations,[4] often producing conflicting values of k_1. These values, obtained by a variety of methods, range over very nearly an order of magnitude. Because of its importance in the chemistry of the atmosphere, the ozone formation reaction continues to be a subject of investigation.[5–8] The reaction is also of importance in the radiation chemistry of oxygen and oxygen-containing systems.[9]

The value of k_1 is determined here by a fast reaction method in which the reaction is initiated by a short-lived perturbation of the system. The method is direct, involving fast optical detection of ozone formation in a homogeneous system. The use of probes or any heterogeneity associated with phase discontinuity is avoided. The result provides a useful addition to the current literature on this reaction.

Experimental

Pulse Irradiation. A 12- to 15-Mev. electron beam from the linear accelerator was used. The maximum current at the cell window was about 80 to 100 ma. The diameter of the electron beam at the cell window was about 15 mm. The pulse duration was generally 1.0 or 0.4 μsec., although a 5-μsec. pulse was used occasionally. General aspects of the experimental arrangement have been described previously.[10]

Irradiation Vessels. The vessels used in this work were designed for the collinear entry of the electron beam at the front window and the analyzing light beam at the rear window. A diagram of the cell is shown in Figure 1 and a photograph in Figure 2. The cell body was made of 304 stainless steel, and the valves were 0.25-in. "speed valves" with "ermeto" connections from Autoclave Engineers Inc. The gasketing arrangement for the aluminum electron beam-window and the quartz light beam-window was similar to that in vessels used in a pulse radiolysis study[11] in which high pressures of hydrogen were needed over a liquid sample. The cell was hydrostatically tested at 200 atm. and was used up to 100 atm. of gas pressure. The cell volume was about 50 cc., of which the pressure gauge section made up 3 cc. and the cold-finger 7 cc.

Spectrophotometry. The technique of spectrophotometric observation of transients was in general the same as described previously.[10,12] An Osram xenon lamp, Type XBO 450W, was used as the source of continuum. Ozone formation was monitored at 2600 Å.[13,14] using a 1P28 photomultiplier. A Bausch and Lomb grating monochromator, Type 33-86-25, f/3.5, was used with grating No. 33-86-01 and a band width of 24 to 70 Å. The light beam passed through the irradiation vessel twice, giving an optical path length of 26 cm. A schematic diagram of the optical system is given in Figure 3. The amplification of the signal from the 1P28 photomultiplier and its display on an

(1) (a) Based on work performed under the auspices of the U. S. Atomic Energy Commission; (b) to whom correspondence should be addressed at the Chemistry Department, The Ohio State University, Columbus, Ohio.
(2) M. S. Matheson and L. M. Dorfman, *J. Chem. Phys.*, **32**, 1870 (1960).
(3) M. C. Sauer, Jr., and L. M. Dorfman, *J. Am. Chem. Soc.*, **86**, 4218 (1964).
(4) For a survey see F. Kaufman, *Progr. Reaction Kinetics*, **1**, 1 (1961).
(5) F. S. Klein and J. T. Herron, *J. Chem. Phys.*, **41**, 1285 (1964).
(6) M. A. A. Clyne, J. C. McKenney, and B. A. Thrush, *Discussions Faraday Soc.*, **37**, 214 (1964).
(7) F. Kaufman and J. R. Kelso, *J. Chem. Phys.*, **40**, 1162 (1964).
(8) F. Kaufman and J. R. Kelso, *Discussions Faraday Soc.*, **37**, 26 (1964).
(9) K. Fueki and J. L. Magee, *ibid.*, **36**, 19 (1963).
(10) L. M. Dorfman, I. A. Taub, and R. E. Bühler, *J. Chem. Phys.*, **36**, 3051 (1962).
(11) J. Rabani and M. S. Matheson, *J. Phys. Chem.*, **69**, 1324 (1965).
(12) G. Czapski and L. M. Dorfman, *ibid.*, **68**, 1169 (1964).
(13) E. C. Y. Inn and Y. Tanaka, *J. Opt. Soc. Am.*, **43**, 870 (1953).
(14) A. G. Hearn, *Proc. Phys. Soc.*, **78**, 932 (1961).

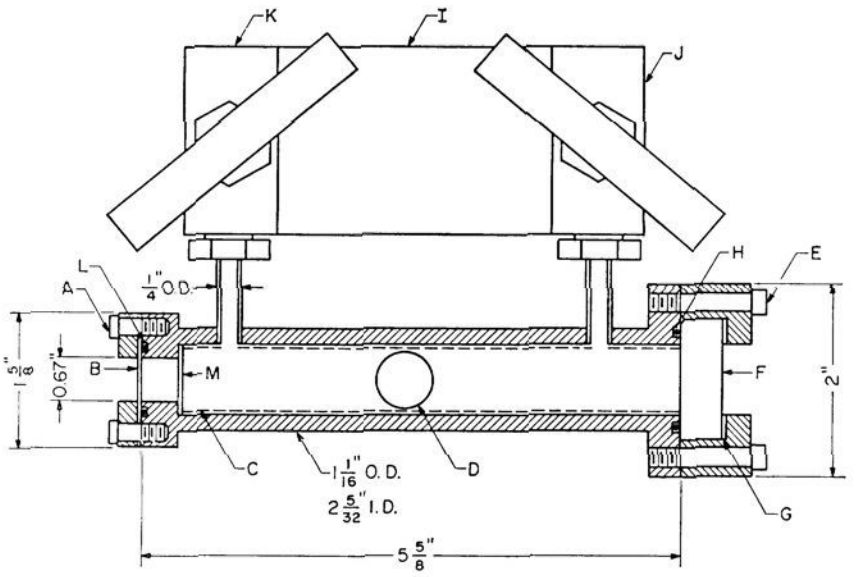

Figure 1. Diagram of high pressure vessel. The vessel was constructed from 304 stainless steel: B, window (6061T6 aluminum), 0.025 in. thick; L, groove, 0.080 in. deep, 0.75-in. i.d., $^{31}/_{32}$-in. o.d., for $^{3}/_{32}$-in. O-ring GRC-27-14; F, window, high purity silica (the inside surface of the window is a few thousandths of an inch below the surface of the holder); G, lead washer, 0.03 in. thick; H, groove, 0.077 in. deep, $^{7}/_{8}$-in. i.d., $1^{5}/_{64}$-in. o.d., for $^{3}/_{32}$-in. O-ring GRC-513-118; M, mirror, 0.5 mm. thick, 0.75-in. diameter quartz, aluminum deposited on surface indicated by arrow; C, dotted line represents stainless steel tube for supporting the mirror (M) (the tube fits snuggly inside the vessel and has a $^{1}/_{32}$-in. wall; the mirror is held in a groove cut into the end of the tube; the fit can be adjusted by means of tabs cut along the sides of the tube); D, arm, $^{1}/_{16}$-in. wall, 0.50-in. o.d., 4 in. long; J and K, high pressure valves (see text) (fittings at top of valves not shown); I, aluminum block to support valves; A, six equally spaced No. 8-32 bolts, with centers on a $1^{3}/_{8}$-in. diameter circle; E, six equally spaced No. 10-32 bolts, with centers on a $1^{5}/_{8}$-in. diameter circle.

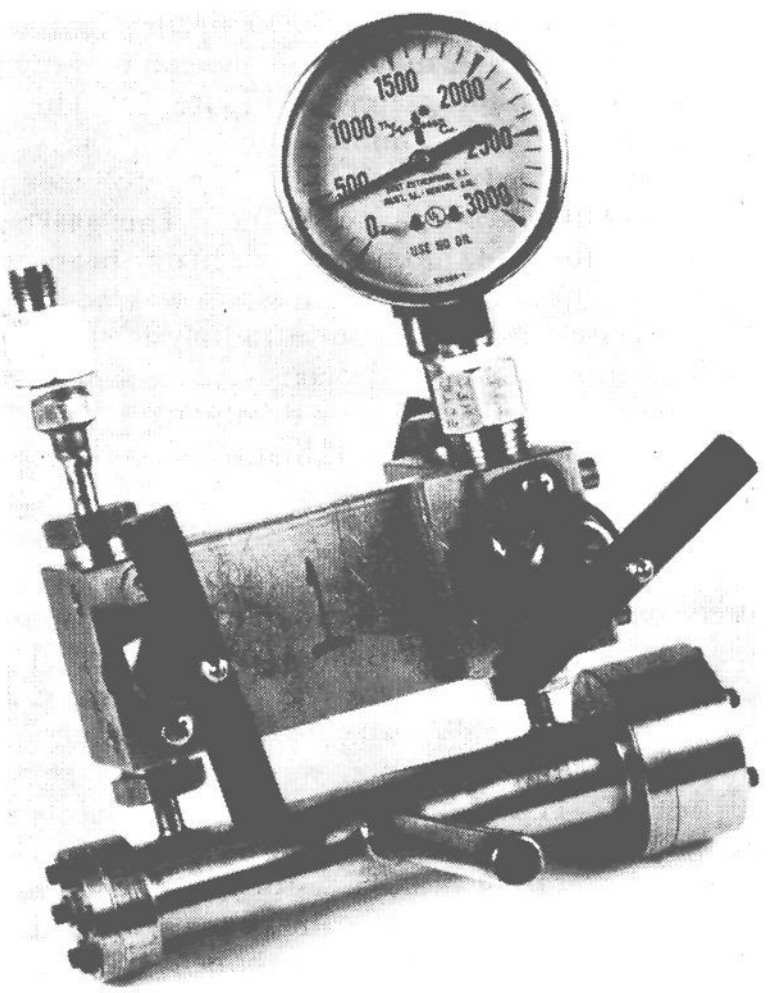

Figure 2. Photograph of high pressure vessel.

oscilloscope have been described.[10] In this work, a Tektronix Type 555 dual-beam oscilloscope was used, and the display on the oscilloscope was photographed using Polaroid Land Picture Roll, 3000 speed/type 47 film. The pictures obtained were enlarged by a factor of two photostatically to facilitate analysis.

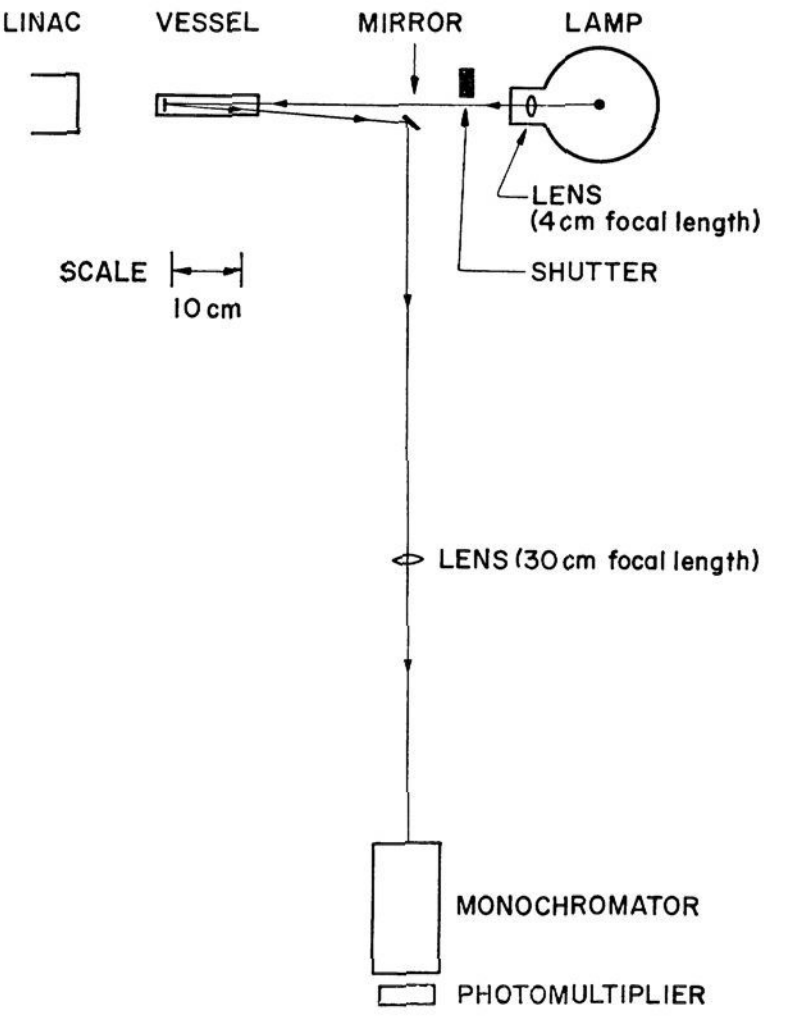

Figure 3. Diagram of optical detection system.

Because of light emission during and slightly after the electron pulse, the first measurements of the formation curves were taken at about 1.5 μsec. after the end of the pulse. Furthermore, every ozone "growth" curve was accompanied by a picture taken with the shutter (see Figure 3) closed so that *only* this emitted light was registered. This "blank" was used to correct the observed growth curve and, in general, was negligible except for the first 10 to 20% of the optical density change of the analyzable portion of the curve.

The light passing through the monochromator was checked for spectral purity using Corning filter 0-52 and was found to contain only about 1% light of longer wave length than that expected from the monochromator setting and slit width.

Materials. The argon was from Linde and the oxygen was from General Dynamics. Both were used without purification. The oxygen was checked for hydrocarbon impurities by gas chromatographic analysis using a flame detector and was found to contain approximately 15 p.p.m. methane. The purity of the argon was stated by the manufacturer as being 7 p.p.m. O_2, 15 p.p.m. N_2, and 5 p.p.m. carbon-containing compounds. Mass spectral analysis of a sample of the argon taken from one of the high pressure vessels filled to about 60 atm. with argon only showed a maximum oxygen content of 20–30 p.p.m. Hydrocarbon impurities in the argon were determined by gas chromatographic analysis using a flame detector. This method actually measures the difference in the impurity contents of the helium carrier gas and the argon sample. The level of hydrocarbon impurities in the helium should be less than 1 p.p.m. according to information from the manufacturer (Bureau of Mines).

No hydrocarbon (C_1–C_4) peaks were detectable in the argon; therefore, the level of such impurities must be less than 1 p.p.m.

Method of Filling Vessels. The vessel was connected to a vacuum system through the two-way valve outlet and to a tank of argon through one of the outlets on the three-way valve (the pressure gauge being on the other outlet; see Figure 2). After evacuation, the valve to the argon tank was closed and the argon tank valve opened. Then oxygen at the desired pressure was let into the vessel from the vacuum system and the valve to the vacuum system was closed. The valve to the argon tank was then opened slightly and argon allowed to fill the vessel until the desired pressure was reached as read on the gauge. The total pressure in the cell was determined independently of the gauge reading by expanding the contents of the cell (of known volume) into a calibrated volume (about 5.5 l.) and measuring the resulting pressure on a manometer. The concentrations of argon and oxygen were known to ±2%.

Results and Discussion

The formation of ozone was monitored at 2600 Å. A typical ozone formation curve is shown in Figure 4. That the absorption was due to ozone was established by spectrophotometric determination of the absorption curve which was found to be in close agreement with the data reported.[13,14]

The value for k_1 was determined as follows. Each rate curve was analyzed by plotting log (log I_{tr}/I_{tr}^f) against time as a test of a first-order rate law. I_{tr} is the light transmitted at 2600 Å. at any time; I_{tr}^f is the light transmitted after the ozone concentration has reached a plateau as evidenced by the plateau in the rate curves. All rate curves showed a well-defined plateau, the rate of disappearance of ozone being substantially lower than its rate of appearance. Figures 4 and 5 show a typical oscilloscope picture and first-order plot.

The plots were linear, and the values for k_1 were obtained from the relationship

$$k_1 = -\frac{2.303S}{[\mathrm{Ar}][\mathrm{O_2}]} \qquad \text{(I)}$$

where S is the slope of the straight line obtained. It may be readily shown that in principle a straight line is to be expected when the data are plotted as described above if the following conditions hold: (1) the production of oxygen atoms is negligible at any time for which a value of I_{tr} is taken from the rate curve; (2) only one precursor is responsible for ozone formation (or the rate constants for the reactions of different precursors are equal); and (3) the time scale of our observed rate curves is such that $t_1(k_{2r} + k_3[\mathrm{Ar}]) >> 1$, where t_1 is the time after the pulse of the first value for I_{tr}. k_2 and k_3 are the rate constants for the reactions

$$\mathrm{O} + \mathrm{O_2} \rightleftarrows \mathrm{O_3}^* \qquad (2)$$

$$\mathrm{O_3}^* + \mathrm{Ar} \longrightarrow \mathrm{O_3} + \mathrm{Ar} \qquad (3)$$

k_{2r} is the rate constant for the reverse reaction 2. Reaction 1 is thought to consist in detail[5] of these two reactions.

The usual steady-state hypothesis may be applied to reactions 2 and 3 if the concentration of the intermediate O_3* is much less than the sum of the concentrations of oxygen atoms and ozone at all times. This will be true if $k_{2r} + k_3[\mathrm{Ar}] >> k_2[\mathrm{O_2}]$. Based on rate constant values in the literature,[5] $k_{2r} + k_3[\mathrm{Ar}]$ is about 10^{10} sec.$^{-1}$, while $k_2[\mathrm{O_2}]$ is about 10^6 sec.$^{-1}$ (for concentrations of O_2 and Ar typical to this work). Therefore, the steady-state hypothesis is applicable here.

Condition 3 above arises from a consideration of the induction period, *i.e.*, the time necessary for the steady state of O_3* to be reached. This can be estimated by integrating the equation $d[O_3^*]/dt = k_2[O][O_2] - k_{2r}[O_3^*] - k_3[Ar][O_3^*]$ with the assumption that [O] is constant during the induction period. Then, setting $d[O_3^*]/dt = 0$, one can solve for the steady-state concentration of O_3*, again under the assumption that [O] is constant. Combining this with the results of the integration leads to the result that the steady state is reached when $(k_{2r} + k_3[\mathrm{Ar}])t >> 1$ which is satisfied if t is about 10^{-8} sec. or greater. Since the time scale of our experiments is about 1000 times greater than this, the steady-state approximation is applicable over the entire time range of the experimental ozone formation curve.

Application of the steady-state approximation that $d[O_3^*]/dt = 0$ leads to the equation

$$\frac{d[\mathrm{O_3}]}{dt} = \frac{k_2k_3}{k_{2r} + k_3[\mathrm{Ar}]}[\mathrm{Ar}][\mathrm{O_2}][\mathrm{O}] \qquad \text{(II)}$$

Our experimental value of k_1 is therefore given by

$$k_1 = \frac{k_2k_3}{k_{2r} + k_3[\mathrm{Ar}]} \qquad \text{(III)}$$

Hence, the experimental value of k_1, when determined as described earlier, should begin to decrease with increasing pressure of argon when the argon pressure is great enough that $k_{2r} >> k_3[\mathrm{Ar}]$ no longer holds. At given concentrations of argon and oxygen the formation of ozone will still be pseudo first order, and a linear plot will be obtained for log (log I_{tr}/I_{tr}^f) *vs.* time.

The values for k_1 and the experimental conditions are shown in Table I. The lower half of the table shows the results from experiments where the filled vessel had been standing at least 20 hr. before pulsing. The reason for this separation is that for samples which

Table I. Rate Constants for $O + O_2 + Ar \rightarrow O_3 + Ar$

—Concentration range— Ar, M	O_2, M × 10^4	No.[a] of expt.	k_1 ± av. dev., M^{-2} sec.$^{-1}$ × 10^{-8}
0.45–0.58	20–124	7	0.83 ± 0.05[b]
0.99–1.12	6.6–107	10	0.78 ± 0.09[b]
2.4–2.6	4.1–70	15	0.76 ± 0.12[b]
3.8–4.3	7–9	7	0.63 ± 0.05[b]
0.45–0.58	20–50	4	0.86 ± 0.05[c]
1.02–1.12	12–26	4	0.77 ± 0.03[c]
2.4–2.6	5–28	4	0.82 ± 0.03[c]
3.8–4.3	7–8	4	0.66 ± 0.06[c]

[a] Each experiment represents analysis of one or more O_3 formation curves using a fresh cell filling. [b] Average of all experiments. [c] Experiments in which samples stood at least 20 hr. before pulsing.

had been standing only 0.5 hr., the apparent rate constant of ozone formation was about 50% less than for samples which had been standing a few hours or more, apparently owing to lack of complete mixing. All of the results in the table were obtained on samples which stood a few hours or more after filling. However, owing to the above observation, the results on samples which stood at least 20 hr. are considered to be more accurate and are used in the following calculations and consideration. The fact that the results from the two halves of Table I are the same within experimental error is, however, significant, for it indicates that complete mixing of the gases takes place in a few hours.

The values of k_1 show no apparent change within experimental precision from [Ar] = 0.5 to 2.5 M, *i.e.*, up to 900 p.s.i., but the value appears to have decreased significantly at [Ar] = 4.0 M. From these data, by plotting $1/k_1$ *vs.* [Ar], we can estimate from the intercept that $k_1 = k_2k_3/k_{2r} = (0.83 \pm 0.08) \times 10^8\ M^{-2}$ sec.$^{-1}$, and from the slope $k_2 = (0.7 \pm 0.5) \times 10^9\ M^{-1}$ sec.$^{-1}$, both at 23°.

The exchange rate for the reaction $O^{18} + O^{16}O^{16} \rightarrow O^{18}O^{16} + O^{16}$ was found to be $0.6 \times 10^9\ M^{-1}$ sec.$^{-1}$ at 37° in a mass spectrometric study[15] of exchange reactions of oxygen atoms. This gives us a more accurate and independent value of k_2. From this value and our experimental value for k_2k_3/k_{2r}, we can estimate the expected decrease in k_1 at [Ar] = 4.0 M. The result is in accord with experiment.

The limiting value of k_1 determined in these experiments, that is, $k_1 = k_2k_3/k_{2r} = (0.83 \pm 0.08) \times 10^8\ M^{-2}$ sec.$^{-1}$, may be compared with values obtained by different methods. Recent publications[7,8] indicate that the rate constant as determined by the "discharge flow" technique has been in error owing to the presence of energetic, metastable species which redissociate O_3, and that the true value for the rate constant, with O_2 as the third body

$$O + 2O_2 \longrightarrow O_3 + O_2 \qquad (4)$$

is $k_4 = (2.7 \pm 0.7) \times 10^8\ M^{-2}$ sec.$^{-1}$, as determined in a flow system where oxygen atoms were produced by thermal decomposition of ozonized purified oxygen. Values of k_4 derived from several studies on the thermal decomposition of O_3 by using the equilibrium constant for reaction 1 derived from thermodynamic properties[16] are $k_4 = 1.5 \pm 0.3 \times 10^8\ M^{-2}$ sec.$^{-1}$. The possible error in the latter value due to the uncertainty in the equilibrium constant (not included in the error limit) is claimed[8] to be easily large enough to explain the discrepancy between the values $k_4 = 2.7 \times 10^5$ and $k_4 = 1.5 \times 10^8$.

We may compare these values for k_4 with our experimental value for k_1 by taking into account the different efficiencies of Ar and O_2 as the third body. It has been reported[17,18] that the third-body efficiency of Ar relative to that of O_2 is 0.6. On this basis we obtain $k_1 = 1.6 \pm 0.4 \times 10^8$ and $k_1 = 0.9 \pm 0.2 \times 10^8$ from the two values for k_4 cited above.

The value of k_1 has recently been determined directly[6] by a discharge flow method in which metastable O_2 molecules were supposedly eliminated, the value obtained being $k_1 = 8.0 \times 10^6 \exp(+1900/RT)$ from 193 to 373°K., which yields $2.0 \times 10^8\ M^{-2}$ sec.$^{-1}$ at 297°K. Also, $k_1 = (1.3 \pm 0.3) \times 10^6\ M^{-2}$ sec.$^{-1}$ was determined[18] in a flow system where oxygen atoms were produced by thermal decomposition of ozonized purified oxygen. We see then that our value, $k_1 = (0.83 \pm 0.08) \times 10^8\ M^{-2}$ sec.$^{-1}$, differs by slightly more than the combined experimental errors with the lower of the two direct determinations of k_1. The difference is also greater than the combined experimental errors for the values cited above and calculated on the basis of the relative O_2–Ar third-body efficiencies, with the exception of the value calculated from thermal decomposition studies.

It is in order that we examine in detail the possible sources of uncertainty in our value for k_1. The possibility exists that oxygen atoms are formed after the pulse by neutralization of ions. This would be expected to yield a low value for k_1. Since neutralization of ions is expected to be a second-order process, the importance of this process in producing oxygen atoms after the pulse relative to oxygen atoms produced by all processes during the pulse should increase for a pulse of constant duration with decreasing current. Variation of the current over a factor of six yielded no variation in k_1. Also, consideration of data on the recombination rate constants for ions indicates that most of the ions are neutralized within 1–2 μsec. after the pulse.[19]

If oxygen atoms were produced after the pulse by the reaction of a long-lived excited state of argon with molecular oxygen, we would expect our experimental value of k_1 to be low compared to the true value. In principle, deviation from linearity would be expected in the plots of experimental data; however, as discussed later, only a large effect would produce a noticeable deviation from linearity. As is discussed later, the plots are linear over a factor of 25 in log (I_{tr}/I_{tr}^f), but this may not be a large enough range to rule out the possibility that metastable argon atoms cause a low value of the rate constant k_1. The only information contained in our experiments which has any bearing on this problem is the fact that the effect of argon pressure on the value of k_1 is small and can be explained entirely on the basis of the transition to second-order kinetics at high argon pressures, as has already been discussed. If metastable argon atoms are important because of $Ar^* + O_2 \rightarrow 2O + Ar$, we expect the experimental value of k_1 to increase, at constant oxygen pressure, with decreasing argon pressure, owing to the different effect of argon pressure on reaction 1 and the latter reaction. If $Ar^* + Ar \rightarrow Ar_2$ occurred, the situation would probably remain unchanged because most of the energy would still be available to dissociate oxygen, either by absorption of light emitted by Ar_2 or by collision of Ar_2 with O_2. Metastable argon atoms would have a negligible effect on k_1 if energy

(15) J. T. Herron and F. S. Klein, *J. Chem. Phys.*, **40**, 2731 (1964).
(16) See ref. 7 for a list of pertinent references.
(17) E. Castellano and H. J. Schumacher, *Z. physik. Chem.* (Frankfurt), **34**, 198 (1962).
(18) F. Kaufman and J. R. Kelso, unpublished results.
(19) Assuming that neutralization of ions occurs by $O_2^- + Ar^+ \rightarrow 2O + Ar$ (k_N), and using the value of $k_N = 1.1 \times 10^{-7}$ cm.^{3}/sec. at 100 atm.[20] for $O^+ + O_2^- \rightarrow 3O\cdot$, we can estimate that under the conditions of our experiments the initial half-time for decay of ions is a few tenths of a microsecond.
(20) Given by K. Fueki and J. L. Magee, *Discussions Faraday Soc.*, **36**, 676 (1963).

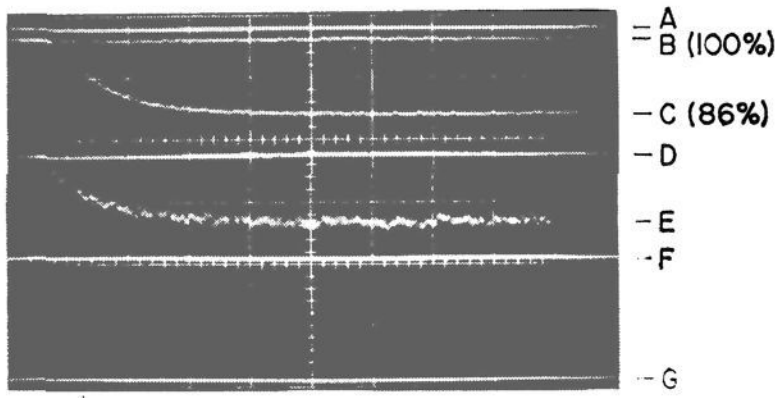

Figure 4. Oscilloscope trace of photomultiplier response. Ozone formation is shown in a vessel containing 1.09 M argon and 1.19 $\times$ 10^{-3} M oxygen. The horizontal scale is 100 μsec. full scale and vertical deflection indicates changes in the signal from the photomultiplier. Two traces were taken simultaneously. A and F are the 100 and 0% transmission lines, respectively, for the upper trace with no amplification. B and C are the 100% line and the ozone formation curve, respectively, for the upper trace amplified 2.5 times. Lines D and G are the 100 and 0% lines for the lower trace with no amplification. E is the ozone formation curve amplified 10 times; its display on the scope was delayed 15 μsec. compared to that of C (the 100% line amplified tenfold does not appear because it had to be set off scale).

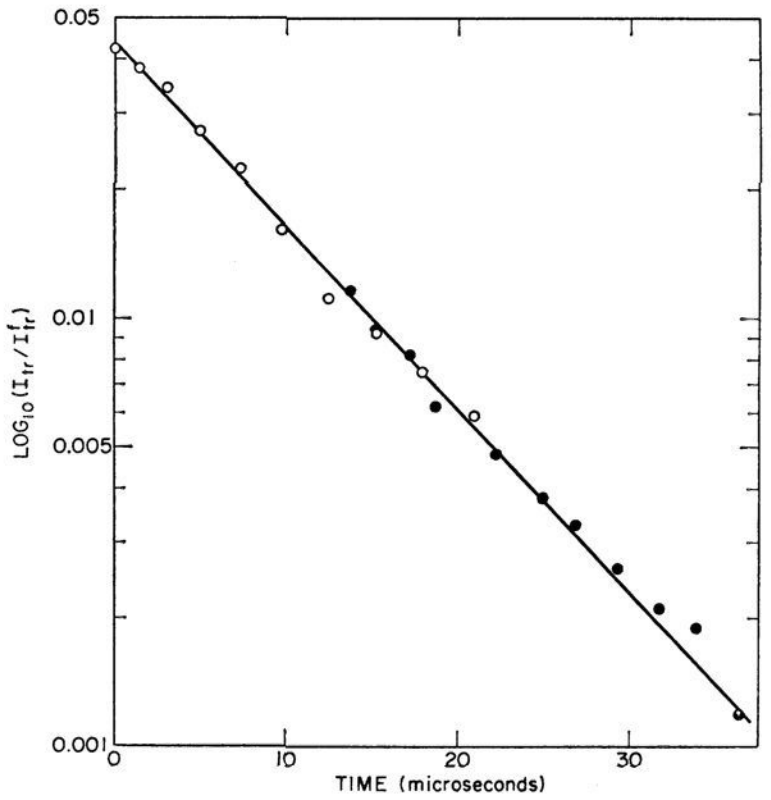

Figure 5. First-order formation plot of curves in Figure 4. The open circles correspond to the upper trace and the filled circles to the lower trace.

transfer between Ar* and O_2 proceeds on every 10 collisions or less.

The experimental value of k_1 would also be low if O_3 were decomposed by reaction with excited oxygen molecules (or other species) simultaneously with the formation of ozone by reaction 1. Occurrence of such reactions can also be ruled out on the basis of experimental evidence. The concentration of ozone produced in a typical pulse is about 10^{-6} M. If the concentration of excited oxygen molecules were similar, the half-time for the reaction $O_2^* + O_3 = O + 2O_2$ would be at least 100 μsec., assuming unity collision efficiency and a collision cross section on the order of molecular dimensions for this reaction. This would have a negligible effect on the ozone growth curves since these had half-times of about 10 μsec. or less. Other evidence against such a reaction is the lack of dependence of k_1 on pulse current or on the concentration of ozone built up in the vessel by successive pulses.

The reactions $O + O + Ar \rightarrow O_2 + Ar$ and $O + O_3 \rightarrow 2O_2$ can be ruled out on the basis of known rate constants[4,21] and would, if they did occur, cause the value of k_1 to be high.

Likewise, impurities in the argon or oxygen which result in the stabilization of oxygen atoms as products other than ozone would lead to a high value of k_1. Such impurities would have resulted in a variation of k_1 with the ratio of argon to oxygen, which was not observed.

It is very likely that the oxygen atoms produced by the pulse radiolysis of argon–oxygen solutions are not all in the (^{3}P) ground state initially. Experimental evidence indicates that O(^{1}D) is deactivated to O(^{3}P) by interaction with many gases.[22-25] Considerations of reactions occurring in the upper atmosphere[23] indicate that the half-time for deactivation of O(^{1}D) in 1 M air would be a few hundredths of a microsecond, and that O(^{1}S) would be deactivated more rapidly. However, this estimate involves a long extrapolation from the low pressures which exist in the upper atmosphere, and furthermore, argon is a very inefficient deactivator of O(^{1}D)[22,24] compared with O_2 or N_2.

The reaction $O(^1D) + O_2 + Ar \rightarrow O(^3P) + O_2 + Ar$ is probably rapid enough to deactivate most of the O(^{1}D) within a few microseconds under the conditions of our experiments. From a study[24c] of the reactions of O(^{1}D) in liquid nitrogen solutions, the estimated rate constant of this reaction is 5×10^9 to 5×10^{10} M^{-2} sec.$^{-1}$. It appears, therefore, that O(^{1}D) will not be important in this work. However, if any significant number of O(^{1}D) (or O(^{1}S)) are not deactivated within a few microseconds after the end of the pulse, we must consider that the observed rate curves represent a combination of the two over-all reactions

$$O(^3P) + O_2 + Ar \longrightarrow O_3 + Ar \quad (1a)$$

$$O(^1D) + O_2 + Ar \longrightarrow O_3 + Ar \quad (1b)$$

In principle, deviation from linearity in the plots of log (log I_{tr}/I_{tr}^f) *vs.* time is expected if the rate curve consists of the two reactions and $k_{1a} \neq k_{1b}$. However, the linearity of such plots is not noticeably affected by small differences in k_{1a} and k_{1b}. For example, unless the rate constant ratio is almost 2, the deviation from linearity is difficult to detect over a factor of 50 in log (I_{tr}/I_{tr}^f) for a 50–50 mixture of O(^{3}P) and O(^{1}D).

The experimental data could be analyzed over a maximum range of about 30 to 50 in log (I_{tr}/I_{tr}^f), which corresponds to a factor of 30–50 in $(D_f - D_1)/(D_f - D_n)$, where D_f is the final optical density of ozone, and D_1 and D_n are the optical densities corresponding to the first and last points taken from a transient curve. Figure 4 shows a typical oscilloscope picture representing the ozone formation. Figure 5 shows a logarithmic plot of log (I_{tr}/I_{tr}^f) *vs.* time using data obtained from the curves in Figure 4. Such plots were always linear over a factor of at least 25 in log (I_{tr}/I_{tr}^f) and often over nearly twice as great a range. Curvature was some-

(21) F. Kaufman and J. R. Kelso, "Chemical Reactions in the Lower and Upper Atmosphere," Interscience Publishers, Inc., New York, N. Y., 1961, p. 255.
(22) S. Sato and R. J. Cvetanović, *Can. J. Chem.*, **36**, 1668 (1958).
(23) M. J. Seaton, *Astrophys. J.*, **127**, 67 (1958).
(24) (a) H. Yamazaki and R. J. Cvetanović, *J. Chem. Phys.*, **39**, 1902 (1963); (b) *ibid.*, **40**, 582 (1964); (c) *ibid.*, **41**, 3703 (1964).
(25) W. DeMore and O. F. Raper, *ibid.*, **37**, 2048 (1962).

times obtained, however, after a factor of 25, in a direction which would be compatible with the presence of two types of oxygen atoms. Even though we feel that this curvature is most likely due to errors in the graphical analysis of the curves, we cannot be certain that the plots are linear over a factor of more than 25 to 30.

Therefore, the participation (to an important extent) of excited oxygen atoms cannot be ruled out because the observed linearity is over an insufficient range. However, from the linearity over the first factor of 25–30 in log (I_{tr}/I_{tr}^{f}), we can say the following: (1) if $k_{1a} > 2k_{1b}$, then initially $O(^3P)/O(^1D) > 3$, and our experimental value is approximately 25% (or less) lower than k_{1a}; (2) if $k_{1b} > 2k_{1a}$, then initially $O(^1D)/O(^3P) > 3$, and our experimental value is approximately 25% (or less) lower than k_{1b}; (3) if $O(^3P)/O(^1D)$ is initially approximately unity, then (a) k_{1a} is less than about $1.8k_{1b}$, and our experimental value is approximately midway between k_{1a} and k_{1b}, or (b) k_{1b} is less than about $1.8k_{1a}$, and our experimental value is approximately midway between k_{1a} and k_{1b}.

One can see that the above statements are valid by making test plots of two simultaneous ozone growth curves, using various values for k_{1a}/k_{1b} and $O(^3P)/O(^1D)$, and adding together the curves due to reactions 1a and 1b. One can then see the extent of nonlinearity expected.

The most reliable value of k_{1a}, as determined[18] by the steady-state flow method already described, appears to be $1.3 \pm 0.3 \times 10^8\ M^{-2}$ sec.$^{-1}$. On the basis of this we can rule out (2) and (3b) above as being possibilities. From (1), our experimental value predicts that $k_{1a} = 0.83 \times 10^8$ to about $1.0 \times 10^8\ M^{-2}$ sec.$^{-1}$, and (3a) predicts from our experimental value that $k_{1a} \simeq 1.0 \times 10^8\ M^{-2}$ sec.$^{-1}$. Within the uncertainty allowed by either (1) or (3a), therefore, there is agreement between the value of k_{1a} obtained from our experiments and the value of $1.3 \pm 0.3 \times 10^8\ M^{-2}$ sec.$^{-1}$, although our results favor the lower extreme of the latter.

Acknowledgments. We are indebted to B. E. Clifft and E. Backstrom for operating the Linac and to E. Klocek and the chemistry machine shop for construction of the high pressure vessels. We are indebted also to Professor F. Kaufman of the University of Pittsburgh for sending us his unpublished results and permission to cite them, and for his helpful comments on this paper.

Chronopotentiometric Diffusion Coefficients in Fused Salts I. Theory[1a]

Richard W. Laity[1b] and James D. E. McIntyre

Contribution from the Frick Chemical Laboratory, Princeton University, Princeton, New Jersey. *Received February 11, 1965*

The significance of the chronopotentiometric diffusion coefficient D_{ch} of an ion in a fused salt solvent is elucidated by developing rigorous equations that relate this quantity to other transport properties of the system ("ordinary" diffusion coefficient and transference numbers). It is shown that when sufficiently small concentrations are employed D_{ch} becomes substantially identical with both ordinary and self-diffusion coefficients. A new method is proposed for taking account of the double layer charging current in determining the "transition time" to be used in the calculation of D_{ch} from experimental chronopotentiograms.

Chronopotentiometry is an experimental procedure in which the potential of an electrode is observed as a function of time during passage of a constant current sufficiently large to produce concentration polarization with respect to a species undergoing electrochemical reaction. In addition to being an analytical tool, the technique has been used to measure a transport parameter usually referred to as the "ionic" diffusion coefficient. Here this will be called the "chronopotentiometric" diffusion coefficient. Its relation to other transport parameters, particularly "ordinary" and "self-diffusion" coefficients, has not been elaborated elsewhere. By developing equations that accurately describe variations of concentration and potential with time in terms of unambiguously defined parameters, the present work will show the physical significance of the chronopotentiometric diffusion coefficient of an electroactive ion in a molten salt solvent.

The Instantaneous Flux. A Rigorous Diffusion–Migration Equation. In any experiment involving ionic migration through a concentration gradient, correct mathematical treatment requires the use of electrochemical potentials as the "thermodynamic forces" on ionic species.[2] A particularly simple set of equations for this purpose is provided by the friction coefficient formalism.[3,4] In applying this approach to steady-state problems in an ionic diffusion layer,[5] the product of concentration times friction coefficient that appears throughout the phenomenological equations was previously expressed in the form $X_k r_{ik}$, where X_k is a kind of mole fraction in which each ionic and molecular species is treated as a separate com-

(1) (a) This work is supported by a contract with the U. S. Atomic Energy Commission; (b) School of Chemistry, Rutgers University, New Brunswick, N. J.

(2) E. A. Guggenheim, *J. Phys. Chem.*, **33**, 842 (1929).
(3) A. Klemm, *Z. Naturforsch.*, **8a**, 397 (1953).
(4) (a) R. W. Laity, *J. Phys. Chem.*, **63**, 80 (1959); (b) *J. Chem. Phys.*, **30**, 682 (1959).
(5) R. W. Laity, *J. Phys. Chem.*, **67**, 671 (1963).